Bioorganic & Medicinal Chemistry Letters xxx (2015) xxx–xxx

Contents lists available at ScienceDirect

Bioorganic & Medicinal Chemistry Letters

journal homepage: www.elsevier.com/locate/bmcl

Discovery of 2-arylamino-4-(1-methyl-3-isopropylsulfonyl-4-pyrazol-amino)pyrimidines as potent anaplastic lymphoma kinase (ALK) inhibitors

Peilong Zhang [a,c], Jiaqiang Dong [b,*], Boyu Zhong [b], Deyi Zhang [b], Can Jin [b], Xuejing Meng [b], Desheng Sun [b], Xiangyuan Xu [b], Yong Zhou [b], Zhi Liang [b], Minghua Ji [b], Hailong Li [b], Tao Xu [b], Guowei Song [b], Ling Zhang [b], Gang Chen [b], Hongbin Yuan [b], Joe Shih [b], Ruihao Zhang [b], Guojun Hou [b], Ying Jin [b], Qiong Yang [b]

[a] Department of Applied Chemistry, Beijing Institute of Technology, Zhongguancun South Street, Beijing 100081, China
[b] Crown Bioscience Inc. (Taicang), 6 Beijing West Road, Taicang Economic Development Area, Taicang 215400, China
[c] Beijing Pearl Biotech Ltd, No. 203, Section 2, Wangjing Lize Zhongyuan, Chaoyang District, Beijing 100102, China

ARTICLE INFO

Article history:
Received 15 April 2015
Revised 27 May 2015
Accepted 5 June 2015
Available online xxxx

Keywords:
ALK
Kinase inhibitor
NSCLC
PK properties
Antitumor efficacy

ABSTRACT

A new series of 2,4-diamino pyrimidine derivatives with a sulfone-substituted pyrazole right side-chain were discovered as potent anaplastic lymphoma kinase inhibitors. Structure–activity relationship of the left side-chain on phenyl substitutions were explored which delivered many potent ALK inhibitors. Among them, **29a** showed favorable pharmacokinetic profiles in rats and dogs together with significant antitumor efficacy in EML4-ALK fusion xenograft model.

Anaplastic lymphoma kinase (ALK) is a receptor tyrosine kinase that belongs to the insulin receptor superfamily, which contains other members such as IGF-1 receptor (IGF-1R), insulin related receptor (IR) and leukocyte tyrosine kinase (LTK). The kinase was firstly identified in 1994 as a part of the nucleophosmin (NPM)–ALK fusion protein found in around 75% of ALK-positive anaplastic large cell lymphoma (ALCL) cases.[1] In adult mice, ALK expression is low and primarily expressed in brain tissue and plays an important role in the development and function of the central nervous system.[2] Although the physiological function of ALK in the normal body is unclear, ALK fusion proteins have been found in many human cancers.[3]

Most recently, ALK has become a hot drug target[4] in cancer therapy along with the identification of the oncogenic fusion gene echinoderm micro-tubule-associated protein-like 4 (EML4)—ALK in around 5% non-small cell lung cancer (NSCLC) patients.[5] Notably, EML4-ALK translocation is almost mutually exclusive with the other oncogenes such as epidermal growth factor receptor (EGFR) and v-Ki-ras2 Kirsten rat sarcoma viral oncogene homolog (KRAS) mutations.[6] Thus the development of selective ALK inhibitors would be a promising treatment option for ALK-driven cancers.

As the first ALK inhibitor approved by FDA in 2011, crizotinib (**1**, PF2341066) was initially designed and developed as a c-Met inhibitor which also showed good antitumor efficacy in ALK-dependent xenograft models.[7] After the initial dramatic responses to crizotinib, however, the patients eventually developed drug resistance within 12 months after treatment with crizotinib. The proposed mechanisms of acquired resistance include secondary (point) mutations (especially for gatekeeper mutation L1196M), ALK gene amplification, and up-regulation of 'ALK-independent' cell-signaling bypass.[8] Now several second generation ALK inhibitors have been or are being developed at different clinical stages,[9] including the second ALK inhibitor ceritinib (**2**, LDK-378) approved by FDA in April, 2014.

The 2,4-diarylamino pyrimidine analogs (DAAPs) were extensively explored in this area, resulting in the discovery of several potent and selective ALK inhibitors (Fig. 1) such as LDK-378 (**2**),[10] NVP-TAE-684 (**3**),[11] AP-26113 (**4**),[12] CEP-37440,[13] etc (among them, the development of **3** was discontinued.[10]). These inhibitors share the common 2,4-diarylamino unit.

* Corresponding author. Tel.: +86 512 3301 1318; fax: +86 512 5387 9801.
E-mail address: dongjiaqiang@crownbio.com (J. Dong).

http://dx.doi.org/10.1016/j.bmcl.2015.06.021
0960-894X/

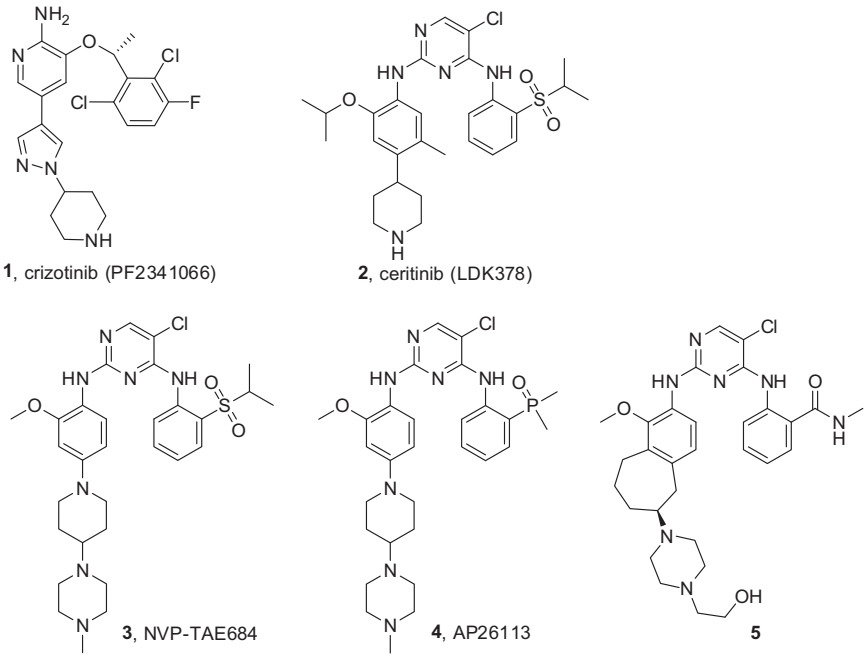

Figure 1. Known ALK inhibitors.

Recently, by applying a bioisosteric strategy, we discovered a series of potent ALK inhibitors with a unique amino pyrazole side-chain replacing 4-aryl on DAAPs scaffold, exemplified by the molecule **6** and **7** (Fig. 2) which showed good in vitro potency against ALK in enzyme and cellular assays.[14]

In the left hand of the structures, there is a structural feature, 4-amino aniline. However, it is generally considered to be a structural alert for creating potential safety liability through the formation of the reactive *p*-diiminoquinone species **A** (Scheme 1). This metabolic liability has been investigated by Novartis[10] and Cephalon[15] during their studies of ALK inhibitors.

To avoid this problem, we decided to optimize our leading compound by moving out N on morpholine (Fig. 3) to deliver a new ALK inhibitor with good anti-tumor efficacy and improved PK properties.

General synthetic routes of new ALK inhibitors are shown in Schemes 2 and 3. The left side-chain anilines were synthesized in several steps. As shown in Scheme 2, SNAr substitution of fluoride **8** with different alcohols in DMF under basic condition afforded **9** in good yield. Intermediate **13** containing fluorine was prepared from phenol **12** through an etherification followed by the nitration using HNO_3. With **9** and **13** in hand, Suzuki coupling followed by catalytic hydrogenation using PtO_2 or Pd/C provided key alkoxy substituted anilines **11a**–**11i**. The intermediates **11j**–**11l** containing trifluoromethoxy, trifluoromethyl and isopropyl groups were obtained from **16** through bromination using NBS, followed by Suzuki coupling and subsequent hydrogenation. Anilines **16** were in turn prepared from starting materials **14**, **15** and **18** respectively. The Negishi coupling between in situ formed organozinc reagent **21** and bromide **9** provided the product **22** with a total 25% yield. The last hydrogenation on **22** afforded aniline **11m**.

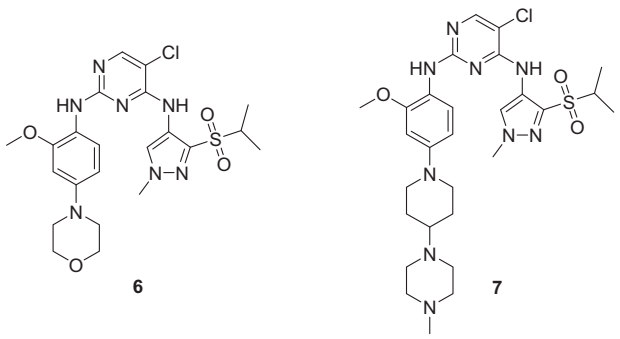

Figure 2. Our early ALK inhibitors.

Scheme 3 summarized the synthesis of the right hand piece and its coupling with the left hand piece to provide the final products. Starting from 3-nitropyrazole **23**, methylation followed by nitration produced dinitro compound **24**. Subsequent nucleophilic substitution by isopropyl thiol, oxidation with *m*-CPBA and reduction of the nitro compound **25** afforded amino pyrazole **26**, which reacted with trichloropyrimidine to provide key intermediate **27**. Buchwald coupling between **27** and amines **11** followed by deprotection afforded desired molecules **28**, which were further functionalized to deliver the final products **29**.

For those compounds containing different $\mathbf{R}^1$ substitution, we firstly evaluated their potency against ALK in enzyme[16] and cellular[17] assays. As shown in Table 1, the simple alkoxy substitution was tolerated and compounds **28b** and **29b** containing cyclopropyloxy displayed the best activities. Slightly bulky substitutions in compounds such as **29c**, **29d** and **29e** diminished the potencies in H2228 cell line. By the comparison between **28a**, **28b** and **29a**, **29b**, N-methylation contributed to improve the activities, especially in cellular assays. In addition, the targets **29f** and **29g** with carbon attached to the phenyl ring directly were 3 to 5 folds less potent, demonstrating the importance of oxygen linkage. Based on the structure of ALK and known literatures,[10,18] we believe that the relatively bulky $\mathbf{R}^1$ substitutions in Table 1 should provide good ALK selectivities and these will be studied in the future.

With the best cyclopropyloxy group set on $\mathbf{R}^1$, the effect of $\mathbf{R}^2$ substitution was then explored. $\mathbf{R}^2$ is at the para-position of $\mathbf{R}^1$ and might have some potential metabolic liabilities. As shown in Table 2, several substitutions were tested against ALK. Molecules **29h** and **29b** with H and Me respectively showed the most potent profiles but **29h** displayed much higher in vivo clearance in rat

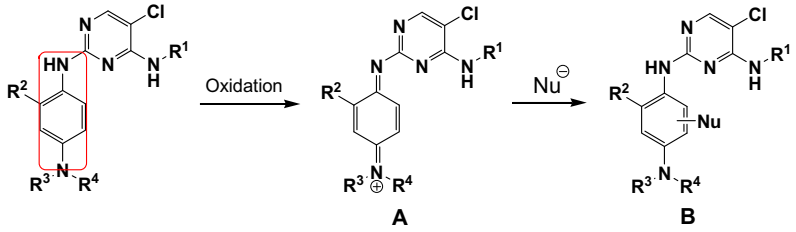

Scheme 1. Metabolic liability of 4-amino aniline through reactive adduct diiminoquinone.

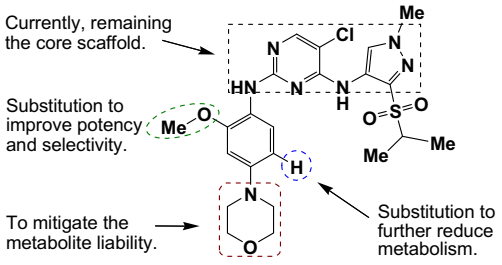

Figure 3. Our SAR strategy.

than **29b** (79.8 vs 22.7 mL/min/kg), possibly due to the existence of the metabolically labile para-H. The substitutions with electro-withdrawing groups such as F, Cl and CN did not improve the potency.

Piperidine substitution in molecule points to the solvent area once bound to the ALK enzyme and SAR on this region is summarized on Table 3. Compared with piperidine, molecules **28l**, **29l**, **28m** and **29m** containing the 4-member and 5-member heterocyclic substitutions showed slightly less potency than **28a** and **28b**. The simple alkylated piperidines such as **29n**, **29o** and **29p** showed very good ALK inhibition while compound **29q** with

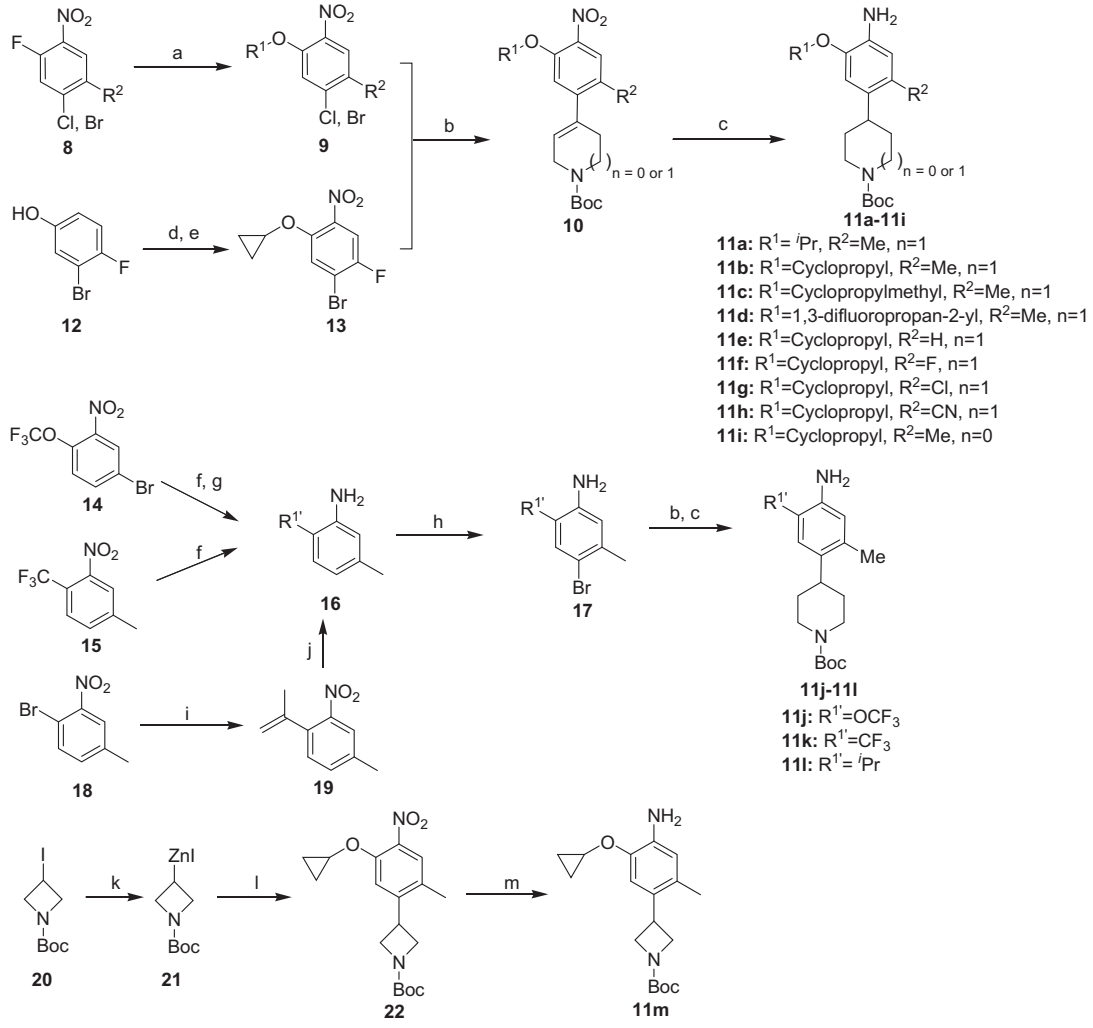

Scheme 2. Reagents and conditions: (a) R_1-OH, ^{t}BuONa, DMF, rt, 85–95%; (b) boronic acid pinacol ester, $Pd(PPh_3)_2Cl_2$, Na_2CO_3, dioxane/H_2O, 100 °C, 80–90%; (c) PtO_2 or Pd/C, H_2, MeOH, rt, 70–85%; (d) cyclopropyl bromide, Cs_2CO_3, KI, NMP, 150 °C, 43%; (e) HNO_3, Ac_2O, −5 °C, 72%; (f) Fe, NH_4Cl, 80 °C, 98%; (g) methyl boronic acid, $Pd(dppf)Cl_2$, K_2CO_3, dioxane, 80 °C, 72%; (h) NBS, DMF, rt, 99%; (i) prop-1-en-2-boronic acid pinacol ester, $Pd(dppf)Cl_2$, $NaHCO_3$, dioxane/H_2O, 95 °C, 85%; (j) Pd/C, H_2, MeOH, rt, 79%; (k) Zn, TMSCl, $BrCH_2CH_2Br$, DMF, 65 °C; (l) **9**, $Pd(dppf)Cl_2$, CuI, DMF, 80 °C, 25% for two steps; (m) Pd/C, H_2, MeOH, rt, 55%.

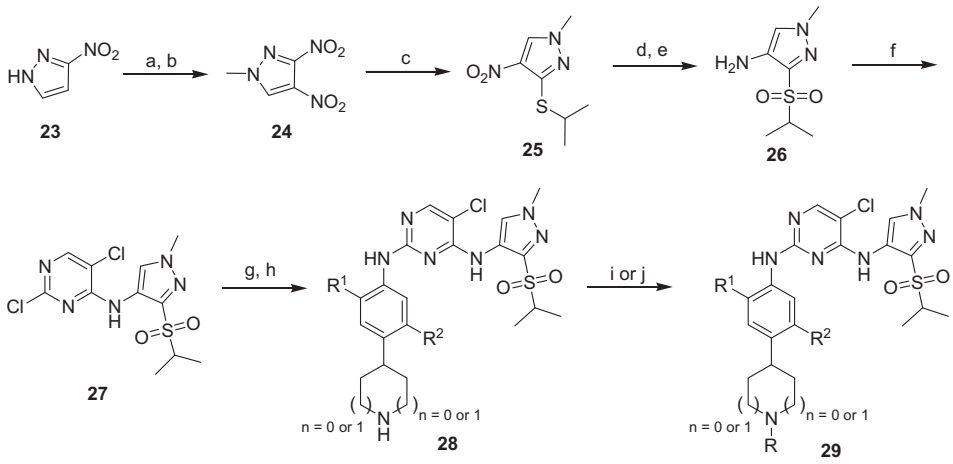

Scheme 3. Reagents and conditions: (a) CH_3I, ^tBuONa, DMF, 0 °C, 92%; (b) HNO_3, H_2SO_4, 100 °C, 79%; (c) isopropyl thiol, K_2CO_3, CH_3CN, rt, 96%; (d) *m*-CPBA, DCM, rt, 98%; (e) Pd/C, H_2, MeOH, rt, 77%; (f) 2,4,5-trichloropyrimidine, Et_3N, EtOH, 70 °C, 70%; (g) **11**, $Pd(OAc)_2$, Xantphos, Cs_2CO_3, THF, sealed tube,130 °C, 20–60%; (h) TFA, DCM, rt, 70–90%; (i) for methylation, HCHO, $NaBH(OAc)_3$, MeOH, AcOH, THF, rt, 50–70%; for **29p**, 3-oxetanone, $NaBH_3CN$, $ZnCl_2$, MeOH, 48 °C, 95%; for other alkylation, RX, K_2CO_3, CH_3CN, 80 °C, 50–85%; (j) for acylation, acyl chloride or isocyanate, Et_3N, DCM, 0 °C–rt, 40–80%.

Table 1
SAR of ortho-substitution of aniline

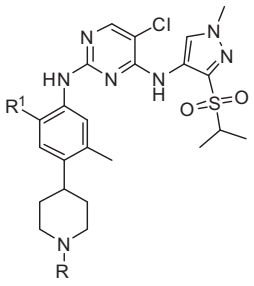

Compound	R^1	R	ALK WT IC_{50} (nM)	ALK (L1196M) IC_{50} (nM)	Karpas-299 cell IC_{50} (nM)	H2228 cell IC_{50} (nM)
28a	^{i}PrO	H	8	20	17	225
29a		Me	4	8	10	96
28b	O	H	2	4	9	122
29b		Me	2	4	6	52
28c	O	H	10	17	43	262
29c		Me	15	48	74	226
29d	F, F, O	Me	10	23	62	403
29e	F_3CO	Me	6	10	20	374
29f	F_3C	Me	22	49	74	1078
29g	^{i}Pr	Me	12	28	–	660

(dimethylamino)ethyl did not improve the potency. Molecules **29r**, **29s** and **29t** containing electro-withdrawing groups also maintained the ALK potency but with much lower in vivo exposure which might be due to stability issue (data not shown). Lastly, the 3-substituted piperidine **29u** demonstrated very good cell activity. However, one enantiomer of **29u** did not show promising in vivo efficacy and the other one displayed unfavorable hERG tolerability.

The pharmacokinetic[19] properties of **29a** were evaluated in rats and dogs and the compound showed favorable clearance, acceptable half life and good bio-availabilities in both species (Table 4). Then this compound was evaluated on a well-established NCI-H2228 (EML4-ALK NSCLC) xenograft model in mice. As shown in Figure 4, compound **29a** showed dose-dependent antitumor efficacy[20] when the animals were treated orally once daily for two weeks. There was almost no anti-tumor inhibition at 3 mg/kg, however, a significant tumor regression was observed at the dose of 30 mg/kg without obvious body weight loss. Notably, almost complete tumor regression at 30 mg/kg was observed after the dosing was stopped for several days.

In summary, we disclosed the discovery of a series of new 2,4-diarylaminopyrimides (DAAPs) with a novel 3-sulfonyl-4-amino pyrazole side-chain as potent ALK inhibitors. We performed extensive SAR exploration on the left hand side of the scaffold and delivered many active compounds displaying nanomolar inhibitory activity against ALK enzymes in wild-type and mutant assays.

Table 2
SAR of R^2 substitution

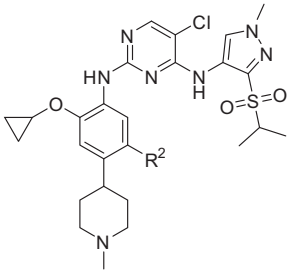

Compound	R^2	ALK WT IC_{50} (nM)	ALK (L1196M) IC_{50} (nM)	Karpas-299 cell IC_{50} (nM)	H2228 cell IC_{50} (nM)
29h	H	3	5	7	36
29b	Me	2	4	6	52
29i	F	3	4	17	125
29j	Cl	4	10	15	103
29k	CN	8	13	100	165

Table 3
SAR of $\mathbf{R^3}$

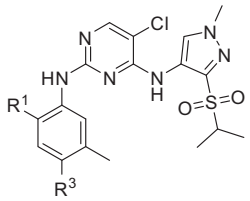

Compound	R^1	R^3	ALK WT IC_{50} (nM)	ALK (L1196M) IC_{50} (nM)	Karpas-299 cell IC_{50} (nM)	H2228 cell IC_{50} (nM)
28l			4	13	60	288
29l		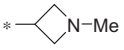	2	5	17	270
28m		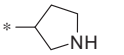	4	5	28	364
29m		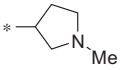	7	4	11	131
29n		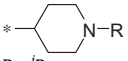 R = ^{i}Pr	2	5	9	58
29o		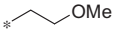	4	7	14	43
29p			10	10	19	44
29q		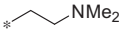	2	5	15	199
29r		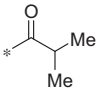	26	29	–	149
29s			9	11	18	59
29t		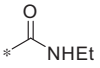	4	6	20	82
29u		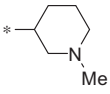	3	7	3	32

Table 4
Pharmacokinetic properties of **29a** in Sprague-Dawley rats and beagle dogs

PK parameters[a]	Rat[b]	Dog[c]
i.v.		
Dose (mg/kg)	1	1
$t_{1/2}$ (h)	5.1	4.9
$AUC_{0-\infty}$ (ng h/mL)	988	637
Vd (L/kg)	7.5	11
CL (mL/min/kg)	16.9	26.2
p.o.		
Dose (mg/kg)	5	3
C_{max}(ng/mL)	199	85.8
t_{max}(h)	6.7	2.0
$AUC_{0-\infty}$ (ng h/mL)	3122	952
F (%)	63.2	49.2

[a] Values are means data from three animals.
[b] Vehicle: DMSO (10%) + 20% HP-β-CD (90%).
[c] Vehicle: 20% HP-β-CD.

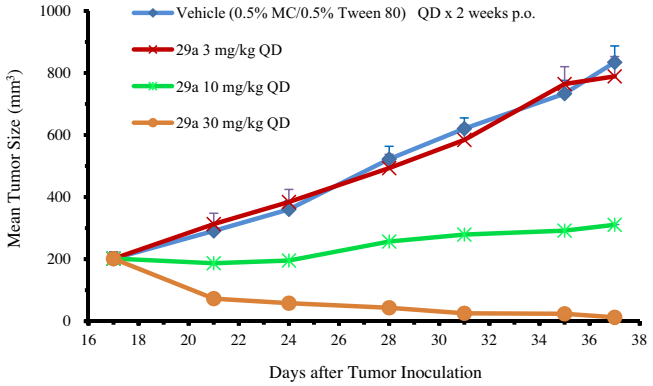

Figure 4. Antitumor efficacy of **29a** in a 14-day mouse H2228 xenograft model.

These compounds also showed very good cell anti-proliferation activity. Compound **29a** showed good pharmacokinetic properties in rats and dogs. Meanwhile, **29a** also demonstrated good dose-dependent anti-tumor efficacy in xenograft mice model. Currently, our efforts toward the identification of a drug candidate are ongoing and the result will be reported in the future.

Acknowledgments

We thank Dr. Shaosong Chu for his pioneer work; Ms. Kefeng Gong for her help in chemical analysis; Dr. QiyongMou for his contribution on side-chain synthesis; Dr. Chengcheng Wang for providing ALK enzymes; Dr. Hepeng Shi for his support and useful discussion.

Please cite this article in press as: Zhang, P.; et al. *Bioorg. Med. Chem. Lett.* (2015), http://dx.doi.org/10.1016/j.bmcl.2015.06.021

Supplementary data

Supplementary data associated with this article can be found, in the online version, at http://dx.doi.org/10.1016/j.bmcl.2015.06.021.

References and notes

1. Morris, S. W.; Kirstein, M. N.; Valentine, M. B.; Dittmer, K. G.; Shapiro, D. N.; Saltman, D. L.; Look, A. T. *Science* **1994**, *263*, 1281.
2. (a) Pulford, K.; Lamant, L.; Morris, S. W.; Butler, L. H.; Wood, K. M.; Stroud, D.; Delsol, G.; Mason, D. Y. *Blood* **1997**, *89*, 1394; (b) Chiarle, R.; Voena, C.; Ambrogio, C.; Piva, R.; Inghirami, G. *Nat. Rev. Cancer* **2008**, *8*, 11.
3. (a) Shaw, A. T.; Engelman, J. A. *J. Clin. Oncol.* **2013**, *31*, 1105; (b) RosKoski, R., Jr. *Pharmacol. Res.* **2013**, *68*, 68.
4. (a) Casaluce, F.; Sgambato, A.; Maione, P.; Rossi, A.; Ferrara, C.; Napolitano, A.; Palazzolo, G.; Ciardiello, F.; Gridelli, C. *Target Oncol.* **2013**, *8*, 55; (b) Galetta, D.; Rossi, A.; Pisconti, S.; Colucci, G. *Expert Opin. Ther. Targets* **2012**, *16*, 45; (c) Mesaros, E. F.; Ott, G. R.; Dorsey, B. D. *Expert Opin. Ther. Pat.* **2014**, *24*, 417.
5. Soda, M.; Choi, Y. L.; Enomoto, M.; Takada, S.; Yamashita, Y.; Ishikawa, S.; Fujiwara, S.; Watanabe, H.; Kurashina, K.; Hatanaka, H.; Bando, M.; Ohno, S.; Ishikawa, Y.; Aburatani, H.; Niki, T.; Sohara, Y.; Sugiyama, Y.; Mano, H. *Nature* **2007**, *448*, 561.
6. (a) Zhang, X. C.; Zhang, S.; Yang, X. N.; Yang, J. J.; Zhou, Q.; Yin, L.; An, S. J.; Lin, J. Y.; Chen, S. L.; Xie, Z.; Zhu, M.; Zhang, X. L.; Wu, Y. L. *Mol. Cancer* **2010**, *9*, 188; (b) Gainor, J. F.; Varghese, A. M.; Ou, S. H. I.; Kabraji, S.; Awad, M. M.; Katayama, R.; Pawlak, A.; Mari, M. K.; Yeap, B. Y.; Riely, G. J.; Iafrate, A. J.; Arcila, M. E.; Ladanyi, M.; Engelman, J. A.; Dora, D. S.; Shaw, A. T. *Clin. Cancer Res.* **2013**, *19*, 4273; (c) Solomon, B.; Shaw, A. T. *Clin. Pharmacol. Ther.* **2014**, *95*, 15.
7. Cui, J. J.; McTigue, M.; Kania, R.; Edwards, M. *Annu. Rep. Med. Chem.* **2013**, *48*, 421.
8. (a) Vijayvergia, N.; Mehra, R. *Cancer Chemother. Pharmacol.* **2014**, *74*, 437; (b) Perez, C. A.; Velez, M.; Raez, L. E.; Santos, E. S. *Lung Cancer* **2014**, *84*, 110.
9. Wang, W. C.; Shiao, H. Y.; Lee, C. C.; Fung, K. S.; Hsieh, H. P. *Med. Chem. Commun.* **2014**, *5*, 1266.
10. Marsilje, T. H.; Pei, W.; Chen, B.; Lu, W. S.; Uno, T.; Jin, Y. H.; Jiang, T.; Kim, S. J.; Li, N. X.; Warmuth, M.; Sarkisova, Y.; Sun, F.; Steffy, A.; Pferdekamper, A. C.; Li, A. G.; Joseph, S. B.; Kim, Y.; Liu, B.; Tuntland, T.; Cui, X. M.; Gray, N. S.; Steensma, R.; Wan, Y. Q.; Jiang, J. Q.; Chopiuk, G.; Li, J.; Gordon, W. P.; Richmond, W.; Johnson, K.; Chang, J.; Groessl, T.; He, Y. Q.; Phimister, A.; Aycinena, A.; Lee, C. C.; Bursulaya, B.; Karanewsky, D. S.; Seidel, H. M.; Harris, J. L.; Michellys, P. Y. *J. Med. Chem.* **2013**, *56*, 5675.
11. Galkin, A. V.; Melnick, J. S.; Kim, S. J.; Hood, T. L.; Li, L. T.; Xia, G.; Steensma, R.; Chopiuk, G.; Jiang, J. Q.; Wan, Y. Q.; Ding, P.; Liu, Y.; Sun, F. X.; Schultz, P. G.; Gray, N. S.; Warmuth, M. *Proc. Natl. Acad. Sci. U.S.A.* **1997**, *104*, 270.
12. The structure of **AP26113** was disclosed at the American Association for Cancer Research annual meeting (at Philadelphia, Apr. 18–22, 2015): Huang, W. S.; Li, F.; Cai, L. S.; Xu, Y. J.; Zhang, S.; Wardwell, S. D.; Ning, Y. Y.; Kohlmann, A.; Zhou, T. J.; Ye, E. Y.; Zhu, X. T.; Narasimhan, N. I.; Clackson, T.; Rivera, V. M.; Dalgarno, D.; Shakespeare, W. C. *AACR* **2015**. Abstract No. 2827.
13. **CEP-37440** might have very similar structure to compound **5** based on the information from Ref. 9.
14. Unpublished results.
15. Mesaros, E. F.; Thieu, T. V.; Wells, G. J.; Zificsak, C. A.; Wagner, J. C.; Breslin, H. J.; Tripathy, R.; Diebold, J. L.; McHugh, R. J.; Wohler, A. T.; Quail, M. R.; Wan, W. H.; Lu, L. H.; Huang, Z. Q.; Albom, M. S.; Angeles, T. S.; Wells-Knecht, K. J.; Aimone, L. D.; Cheng, M. G.; Ator, M. A.; Ott, G. R.; Dorsey, B. D. *J. Med. Chem.* **2012**, *55*, 115.
16. Enzyme inhibition assays: the ALK WT activity was determined in a 384-well HTRF format using HTRF® KinEASE™-TK Assay Kit (Cat# 62TK0PEC, Cisbio) and recombinant human ALK enzyme (Cat# ALK-20110607,Crownbio). The final assay conditions were 50 mM HEPES (pH 7.0), 0.02% NaN_3, 0.01% BSA, 0.1 mM Orthovanadate, 5 mM $MgCl_2$, 1 mM DTT, 1 μM TK Substrate-biotin, 20 μM ATP, 40 nM SEB reagent and 10 ng ALK WT enzyme, TK Substrate-biotin and SEB reagent were provided by Cisbio kit. The assay reaction time was 30 min after which the antibody detection mix was added. The L1196M mutant ALK enzyme assay was done in a similar format, mutant enzyme was from Crownbio (Cat# ALKm-20110923) and 5 μM ATP was used in the assay buffer. IC50 was calculated by Xlift software using four-parameter logistic concentration–response curve.
17. Cell anti-proliferation assay: cells were seeded in 96-well tissue culture plate, and incubated at 37 °C, 5% CO_2 for 2 hours, then cells were exposed to various concentrations of compounds and further cultured for 96 h. Cell proliferation was determined using CellTiter-Glo assay kit (Promega, G7572). IC_{50} was calculated by Xlift software using four-parameter logistic concentration–response curve.
18. Kinoshita, K.; Kobayashi, T.; Asoh, K.; Furuichi, N.; Ito, T.; Kawada, H.; Hara, S.; Ohwada, J.; Hattori, K.; Hong, W. S.; Park, M. J.; Takanashi, K.; Tsukaguchi, T.; Sakamoto, H.; Tsukuda, T.; Oikawa, N. *J. Med. Chem.* **2011**, *54*, 6286.
19. PK studies: **29a** (mesylate salt) was formulated as a solution in DMSO (10%) and 20% HP-β-CD (90%) and it was administrated to male Sprague-Dawley rats ($n = 3$ per group) by intravenous (i.v., 1 mg/kg) or oral (p.o., 5 mg/kg). After dosing, blood samples were collected at 0.08, 0.25, 0.5, 1, 2, 4, 6, 8, 24 h for i.v. dosing and at 0.25, 0.5, 1, 2, 4, 6, 8, 24 h for p.o. dosing. The samples were centrifuged and the collected plasma was analyzed by LC–MS/MS. The PK parameters were calculated by Winnonlin 6.3 software Non-Compartmental model. **29a** (mesylate salt) was formulated as a solution in 20% HP-β-CD and it was administrated to male beagle dogs ($n = 3$ per group) by intravenous (i.v., 1 mg/kg) or oral (p.o., 3 mg/kg). Sample collection and analysis followed the same method as above.
20. In vivo efficacy: Balb/c nude mice inoculated with H2228 were randomized into four groups (8 mice per group) with an average tumor volume of around 200 mm^3. Then the mice were dosed by vehicle and **29a** (mesylate salt, formulated in 0.5% MC and 0.5% Tween 80, oral, QD) at dose levels of 3, 10 and 30 mg/kg. Mice were monitored for the behavior and body weight loss, and tumors were measured twice weekly in two dimensions using a caliper, and the volume is expressed in mm^3 using the formula: $V = 0.5\ a \times b^2$ where a and b are the long and short diameters of the tumor, respectively. Tumor growth was calculated by $T/C\% = (T - T_0)/(C - C_0) \times 100$, where T and T_0 are the mean tumor volumes on a specific experimental day and on the first day of treatment respectively for the treatment groups, where C and C_0 are the data for the control group. Meanwhile, tumor growth inhibition (TGI) was calculated by $TGI = (1 - T/C) \times 100\%$.